




Article

Long-Term Stability Evaluation and Pillar Design Criterion for Room-and-Pillar Mines

Yang Yu ¹ , Shen-en Chen ², Ka-zhong Deng ^{1,*}  and Hong-dong Fan ^{1,3} 

¹ School of Environment Science and Spatial Information, China University of Mining and Technology, Xuzhou 221116, China; yuyang1989cumt@gmail.com (Y.Y.); cumtfhd@163.com (H.-d.F.)

² Department of Civil and Environmental Engineering, University of North Carolina at Charlotte, 9201 University City Blvd., Charlotte, NC 28223, USA; schen12@uncc.edu

³ State Key Laboratory of Geohazard Prevention and Geoenvironment Protection, Chengdu University of Technology, Chengdu 610059, China

* Correspondence: kzdeng@cumt.edu.cn; Tel.: +86-0516-8388-5986

Received: 15 September 2017; Accepted: 16 October 2017; Published: 18 October 2017

Abstract: The collapse of abandoned room-and-pillar mines is often violent and unpredictable. Safety concerns often resulted in mine closures with no post-mining stability evaluations. As a result, large amounts of land resources over room-and-pillar mines are wasted. This paper attempts to establish an understanding of the long-term stability issues of goafs (abandoned mines). Considering progressive pillar failures and the effect of single pillar failure on surrounding pillars, this paper proposes a pillar peeling model to evaluate the long-term stability of coal mines and the associated criteria for evaluating the long-term stability of room-and-pillar mines. The validity of the peeling model was verified by numerical simulation, and field data from 500 pillar cases from China, South Africa, and India. It is found that the damage level of pillar peeling is affected by the peel angle and pillar height and is controlled by the pillar width–height ratio.

Keywords: room-and-pillar mining; long-term pillar stability; pillar degradation; mine safety; pillar design

1. Introduction

The room-and-pillar mining method is widely used in many coal producing countries, including the U.S., China, India, and South Africa [1–4]. Compared with other underground mining methods, room-and-pillar mining can effectively control ground subsidence and minimize the effects on the surface structure [5,6]. However, the collapse of a single pillar in the mine shaft can cause load transfer to the neighboring pillars and subsequently results in ground subsidence at the surface. In some cases, cascading pillar failures or sinkholes may result if the neighboring pillars cannot carry the additional load, or if the resulting roof span is too large for effective load transfer [7–12]. Post-pillar-failure disasters, such as collapse-induced earthquakes and non-uniform ground subsidence may also appear during, or after, mining activities, threatening the safety of people and infrastructures [2,7,11]. The literature indicates that the pillar failure may occur in a couple of hours or decades after mine abandonment [5,13–15]. The long-term stability means that the coal pillar can be stable in the long-term after the mining panels or coal mines are closed, and there will be no ground subsidence or post-mining damages on the ground surface structures that are induced by pillar instability.

Since the width–height ratio of pillars is smaller in room-and-pillar mines, pillar failures appear more frequently in room-and-pillar mining than stripe mining. Records of U.S. pillar failures showed that the pillar failures are usually accompanied by sudden roof subsidence, pillar spalling, or floor heave, and such failures appear more frequently when width–height ratios of pillars are smaller than 3 for coal mines, less than 2 for non-metal mines, and less than 1 for metal mines [7]. The experiences

from South Africa and Australia also showed that the coal pillars with low width–height ratio have better tendency to collapse with time [14,16]. It is concluded that the collapses of slender pillars with width–height ratio ranging from 3 to 4 will be brittle and may lead to cascading pillar failures, the failures of intermediate pillars with width–height ratios of 4–8 will make the pillars “squeeze” to non-violent rib spalling and, finally, the squat pillars with width–height ratios larger than 8 will hardly fail [14,17].

Studies on the long-term stability of mineral pillars showed that, over time, weathering and stress will eventually result in pillar size reduction and pillar strength degradation [18–21]. The dissolution of minerals in rock-like materials, for example, may reduce the effective size of mineral pillars [19], or may increase the micro cracks and damages in the material, leading to low-stress material failures [22]. Some mineral partings in coal pillars are more sensitive to water and will peel from the pillar, reducing the pillar size [18]. On the other hand, high overburden stress can cause progressive rib spalling of pillars [20]. Such progressive pillar failure resulting from the coupled effects of weathering and stress is defined as pillar scaling or pillar peeling.

To predict pillar life, a constant pillar scaling rate has been proposed by Van der Merwe [13,23] and Sami et al. [21]. However, because of the complicated coupling effect of weathering and stress, the constant pillar scaling rate is empirical, site-specific, and difficult to obtain reliable results on pillar stability or pillar life. Salamon [24] suggested that the coal debris spalled from pillar ribs during peeling can restrict the further scaling of a coal pillar, and propose a pillar peeling model, which can be used to calculate the ultimate scaling of the pillar. Backfill mining experiences indicate that the confinement of the non-cohesive backfill can restrict the pillar dilating and may enhance pillar strength, providing support to Salamon’s concept [25,26].

Considering the size reduction and peeling behaviors of coal pillars, this paper proposes a conservative pillar peeling model. The peeling model assumed that a pillar will slowly peel off as long as the pillar rib is not covered by loose coal debris piles. Thus, it represents the worst case scenario of a pillar. The effects of peeled coal debris pile on coal pillar stability are investigated by numerical simulations. The peeling model is verified by 500 failed and stable pillar cases. Finally, failure of a single pillar on the stability of surrounding pillars are analyzed, and a long-term stability evaluation method is proposed.

2. Coal Pillar Peeling Model

As long as the pillar rib is exposed to the environment without horizontal confinements, it will suffer from the long-term exposure to weathering and stress. The pillar rib may slowly peel off and the pillar size may scale down because of such effects. The coal debris spalled from the pillar rib during the peeling process will accumulate around the coal pillars, providing a volume restriction to the coal pillars and protecting the internal pillar rib from further environmental weathering. Figure 1 shows some engineering cases about distribution of coal debris around peeling pillars [2].

Salamon [24] first proposed a pillar peeling model for square pillar to describe this situation and assumed that the pillar is scaling down uniformly towards the pillar center. The peeled coal debris then accumulates around the pillar and forms a triangle pile. The peeling progress will stop if the coal debris pile fully covers the coal pillar. However, the assumption of uniformly peeling may underestimate the maximum peeling depth in the coal pillars—the peeling at the pillar bottom is less than that at pillar top. On the other hand, the laws of pillar rib spalling indicated that the rib spall appear more frequently near the pillar top, and the possibility of spalling increases as the pillar height increases [27–29]. It is, therefore, more reasonable to assume a non-uniform pillar peeling model to make a safer stability evaluation.

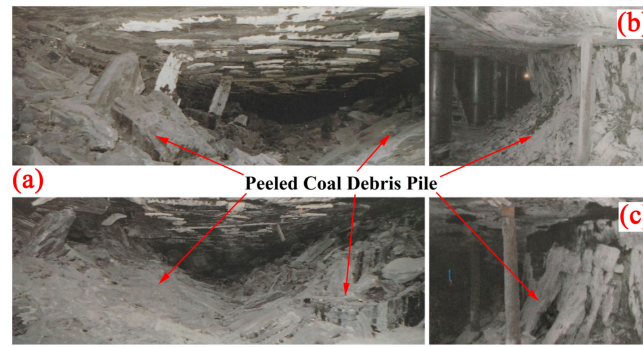


Figure 1. Examples of coal pillar spalling and coal fragment pilling up in the U.S. [2]: (a) failed pillars in the Cedar Grove coal seam: the coal fragments accumulated around the failed pillars and prevented them from totally crushing; (b) rib spalling of an airway pillar in the Hiawatha coal seam; and (c) rib spalling of yielding pillar in the Hiawatha coal seam.

Figure 2 shows the diagram of a non-uniform peeling model where the shape of the peeled coal debris is affected by the room width: a triangle pile will form if the room width is large (an isolated pillar case, Figure 2a), whilst the coal debris from two pillars will overlay each other if the room width is small (a non-isolated pillar case, Figure 2b). Assuming that the peeling of the coal pillar is non-uniform towards the pillar center and the peeled cross-section can be represented by a quarter of an ellipse—the semi-major axis of the ellipse will represent the pillar height and the semi-minor axis represents the maximum peeling depth on the pillar.

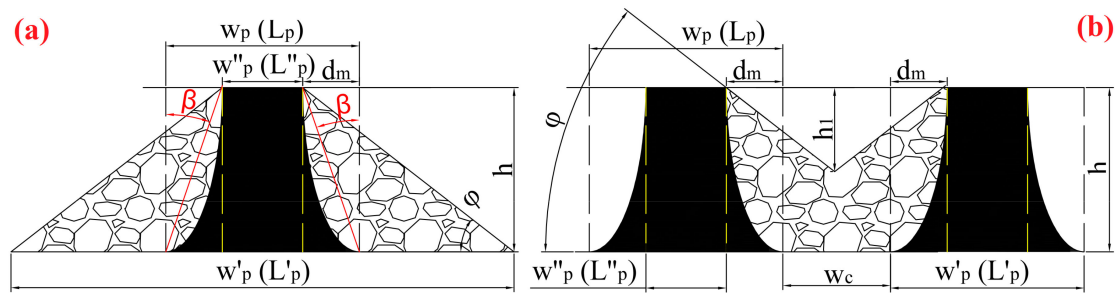


Figure 2. The diagram of pillar peeling for (a) an isolated pillar and (b) non-isolated pillars.

For an isolated rectangle pillar, the spalled coal debris are the granular materials piling up around the pillar in a triangle shape, the progressive peeling will stop if the coal debris pile reach the pillar top and the bottom angle of the pile will approximate the repose angle φ . Equations (1)–(5) can be proposed based on the geometry in Figure 2a:

$$f = \frac{1}{\tan \varphi}, \quad (1)$$

$$w''_p = w_p - 2d_m, \quad (2)$$

$$L''_p = L_p - 2d_m, \quad (3)$$

$$w'_p = 2fh + w_p - 2d_m, \quad (4)$$

$$L'_p = 2fh + L_p - 2d_m, \quad (5)$$

where φ is the repose angle, $^\circ$; d_m is the maximum peeling depth on a single side of a pillar; w_p and L_p are the initial pillar width and pillar length respectively; w''_p and L''_p are minimum pillar width and pillar length after peeling; h is the pillar height; w'_p and L'_p are the bottom width and bottom length of the trapezoidal column.

The pillar peeling process can be assumed as four elliptical cylinders cutting through the coal pillar; thus, the total volume of peeled parts on coal pillar V_{peel} and the volume of the residual pillar V_{res} can be calculated:

$$V_{peel} = \frac{\pi}{2}(w_p + L_p)hd_m - \frac{8}{3}hd_m^2, \quad (6)$$

$$V_{res} = V_p - V_{peel} = w_p L_p h - \frac{\pi}{2}(w_p + L_p)hd_m + \frac{8}{3}hd_m^2, \quad (7)$$

and the volume of the trapezoidal column V_1 is:

$$V_1 = \frac{h}{6} [w_p'' L_p'' + w_p' L_p' + 4(fh + w_p'')(fh + L_p'')], \quad (8)$$

The peeled volume of coal pillar V_{peel} will increase with a bulk factor, k , and equals the volume of the peeled coal debris pile:

$$kV_{peel} = V_1 - V_{res}, \quad (9)$$

Combining Equations (1)–(9), the maximum peeling depth can be calculated as:

$$[4 + \frac{8}{3}(k-1)]d_m^2 - \{4fh + [2 + \frac{\pi}{2}(k-1)](L_p + w_p)\}d_m + \frac{4f^2h^2}{3} + fh(L_p + w_p) = 0, \quad (10)$$

Define the minimum room width leading to an isolated pillar as the critical room width w_{CD} , then:

$$w_{CD} = w_p' - w_p = L_p' - L_p = 2fh - 2d_m, \quad (11)$$

Figure 2b shows the case when the room is smaller than the critical room width. For a single pillar, the combination of the residual pillar and the coal debris pile consists of a trapezoidal column and a rectangle cube base, and the following can be used:

$$fh_1 = d_m + \frac{w_c}{2}, \quad (12)$$

$$V_2 = \frac{h_1}{6} [w_p'' L_p'' + (w_p + w_c)(L_p + w_c) + 4(fh_1 + w_p'')(fh_1 + L_p'')] + (h - h_1)(w_p + w_c)(L_p + w_c), \quad (13)$$

$$kV_{peel} = V_2 - V_{res}, \quad (14)$$

where w_c is the room width, m; V_2 is the total volume of the trapezoidal column and the rectangle cube base, m³.

Combining Equations (1)–(7) and Equations (12)–(14), the maximum peeling depth when the room width is smaller than w_{CD} can be calculated as:

$$\begin{aligned} & \frac{4}{3f}d_m^3 + \left(\frac{8h(k-1)}{3} - \frac{L_p + w_p}{f}\right)d_m^2 + \left[\frac{L_p w_p}{f} - \frac{(L_p + w_c)(w_p + w_c)}{f} + \frac{\pi h(L_p + w_p)}{2}(1-k)\right]d_m + \\ & \frac{w_c}{12f}[L_p w_p + (L_p + w_c)(w_p + w_c) + (w_c + 2w_p)(w_c + 2L_p)] + h(L_p + w_c)(w_p + w_c) - \\ & \frac{w_c}{2f}(L_p + w_c)(w_p + w_c) - L_p w_p h = 0, \end{aligned} \quad (15)$$

Thus, the maximum peeling depth of pillar for all conditions can be determined by Equations (10), (11), and (15). When the room width is larger than the critical room width w_{CD} , Equation (10) should be used, otherwise, Equation (15) should be used.

3. Effects of Pillar Width–Height Ratio on Pillar Peeling

According to Figure 2, the maximum peeling depth d_m can also be represented by the peeling angle β , which reflects the degree of peeling damage on a pillar: The larger β is, the more severe the peeling damage will be. Considering the $L_p = w_p$ case, as the pillar will totally peel when $d_m = w_p/2$, the maximum peeling angle β_m that a pillar can bear is:

$$\frac{d_m}{h} = \frac{w_p}{2h} = \frac{R}{2} = \tan \beta_m, \quad (16)$$

Equation (16) indicates that β_m is only related to the pillar width–height ratio. A pillar with a large width–height ratio has a larger β_m , and has a better ability to resist the pillar peeling.

Using β to represent d_m , Equations (10), (11), and (15) can be transformed as:

$$\frac{d_m}{h} = \frac{2f}{m_1} + \frac{m_2 R}{m_1} - \sqrt{\left(\frac{2f}{m_1} + \frac{m_2 R}{m_1}\right)^2 - \frac{4f^2}{3m_1} - \frac{2fR}{m_1}} = \tan \beta, \quad (17)$$

$$R_{CD} = \frac{w_{CD}}{h} = 2f - 2\left(\frac{2f}{m_1} + \frac{m_2 R}{m_1} - \sqrt{\left(\frac{2f}{m_1} + \frac{m_2 R}{m_1}\right)^2 - \frac{4f^2}{3m_1} - \frac{2fR}{m_1}}\right), \quad (18)$$

$$\frac{4}{3f}(\tan \beta)^3 + \left(\frac{8(k-1)}{3} - \frac{2R}{f}\right)(\tan \beta)^2 + \left[\frac{R^2}{f} - \frac{(R+R_c)^2}{f} + \pi(1-k)R\right]\tan \beta + \left\{\frac{R_c}{12f}[R^2 + (R+R_c)^2 + (2R+R_c)^2] + (R+R_c)^2 - \frac{R_c}{2f}(R+R_c)^2 - R^2\right\} = 0, \quad (19)$$

where R is the initial width–height ratio of pillar; R_{CD} is the critical width–height ratio of the room m_1 and m_2 coefficients related to bulking factor k . $m_1 = 4 + 8(k-1)/3$, $m_2 = 2 + \pi(k-1)/2$, and $R = L_p/h = w_p/h$.

β is only related to the repose angle, bulk factor, and width–height ratios of the pillar and room. Figure 3a,b shows the relationships between the peeling angle β and width–height ratio of an isolated pillar. β will exponentially increase when the pillar width–height ratio is smaller than 3, which explains why the cascading pillar failures occur more frequently for slender pillars: slender pillars have smaller β_m and larger β and will result in severe peeling damages when β is reached or exceeds β_m . Increases of the bulk factor and repose angle can significantly decrease β , which means the stronger and stiffer the pillar is, it can have a better ability to resist the peeling process. This offers the explanation of why the pillar width–height ratio leading to cascading pillar failures is smaller than 2 for non-metal mines, but is smaller than 3–4 for coal mines [7]. The bulk factor is usually 1.6–1.8 for sandstone and is usually smaller than 1.3 for coal. If a coal pillar and a sandstone pillar have the same width–height ratio, then β of the sandstone pillar is significantly smaller than the β of the coal pillar (Figure 3a), and the peeling damage will be more severe on the coal pillar. Figure 3c shows the relationships between the peeling angle β and width–height ratio of non-isolated pillars: β decreases if the room width decreases. However, such a decrease is not obvious when the pillar width–height ratio is small.

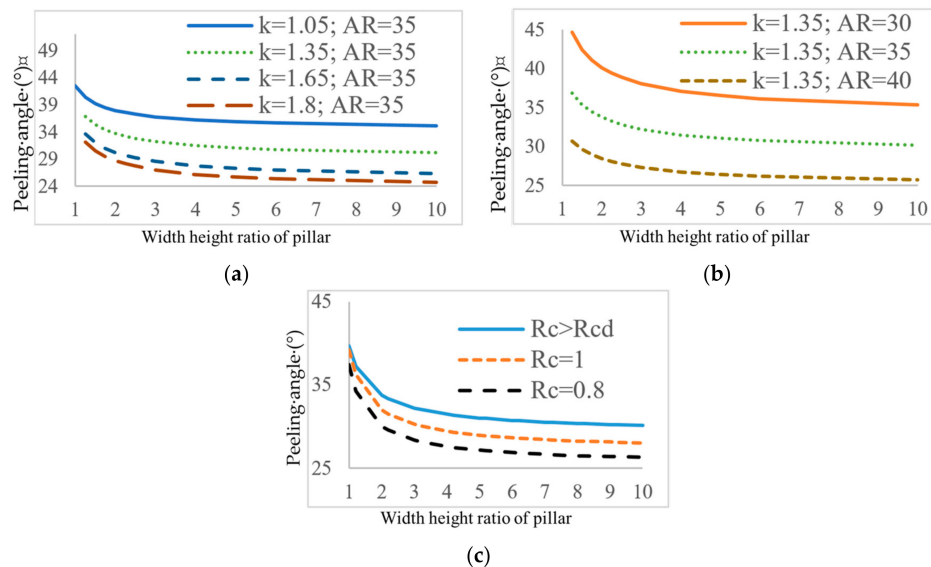


Figure 3. The relationship between the peeling angle and the width–height ratio of the pillar: k for bulk factor; AR for angle of repose; $^\circ$; R_c and R_{cd} for room width–height ratio and critical room width–height ratio. For (a,b), the room width is larger than the critical room width; and for (c), the room width is smaller than the critical room width, $k = 1.35$; $AR = 35^\circ$.

4. Effect of Peeled Debris Pile on Pillar Stability

To study the effect of peeled coal debris pile on pillar stability, UDEC is used to model peeling pillars. The Mohr-Coulomb failure criterion is assumed for material failures. The numerical model has two pillars, in which one pillar was surrounded by triangle-shaped, peeled debris piles and the other pillar was just a single pillar (Figure 4a). For simplicity, we assume that the piles consist of rigid coal fragments and the coal fragments in the pile are only affected by internal frictions. The properties of the coal fragments are the same as of the coal pillars, but the interface strength between the coal fragments is assumed to be zero. The model base is fixed and the pillars are covered by sandstone roofs. Overburden pressure is represented by a static vertical stress of 1.1 MPa applied on the top of the sandstone roof. The mechanical properties of the model are adopted from the Yulin mining area in China [30] and are listed in Table 1. The element size of the model is 0.2 m. Static equilibrium analysis is then conducted with consideration of gravity loading to the system.

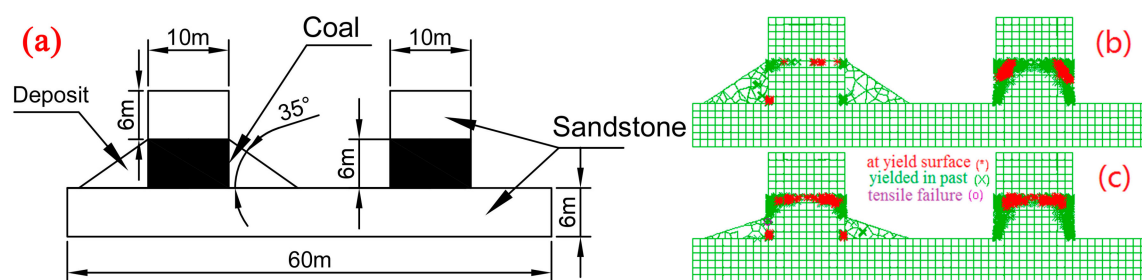


Figure 4. The numerical simulation design and results: (a) scheme of model prototype; (b) simulation result that the pile height equals to the pillar height; and (c) simulation result that the pile height is smaller than the pillar height.

Table 1. Mechanical properties of the model.

Material	Density (kg/m ³)	Elastic Modulus (GPa)	Poisson Ratio	Internal Friction Angle, (°)	Cohesion, (MPa)	Tensile Strength, (MPa)
Coal	1290	2.196	0.27	42	2.61	0.72
Sandstone	2370	15.093	0.15	34.6	11.6	6.36
Debris pile	1290	2.196	0.27	42	2.61	0.72
Coal-sandstone Interface	-	-	-	42	2.61	0.72
Coal fragment Interface	-	-	-	42	0	0

Figure 4b,c show the simulation results which indicate that the yielding of the pillars caused by overburden stress is more severe at the pillar top. This means the non-uniform peeling assumption is reasonable. As the pillar peels away slowly, the actual stress on the pillar gradually increases and the yield zone of the pillar increases, eventually leading to pillar failure. The yield zone is reduced if the pillar is surrounded by a coal debris pile, which restricts the horizontal deformation of the coal pillar, and the stress condition is closer to a triaxial stress state instead of a uniaxial stress state (Figure 4b). The decrease of the debris pile height will expand the yield zone in the pillar, but the overall stability of the pile-affecting pillar is still better than the single pillar (Figure 4c). Therefore, the peeling progress can be considered to stop when the pile height equals to the pillar height, because the further development of yielding areas would cease and the pillar strength is enhanced.

5. Application of the Peeling Model in Case Studies

Mine data on 354 stable and 145 failed pillars have been collected from China [31], South Africa [13,15,16], and India [1,32]. The stability of these pillars are evaluated and discussed in the following:

The initial stress (PS_0) on pillars and their initial safety factors (SF_0) can be calculated by tributary area theory, and the initial pillar strengths (S_0) are estimated by the Salamon formula:

$$PS_0 = \rho g H \frac{(w_p + w_c)^2}{w_p^2}, \quad (20)$$

$$S_0 = \sigma \frac{w_p^{0.46}}{h^{0.66}}, \quad (21)$$

$$SF_0 = \frac{S_0}{SP_0}, \quad (22)$$

where ρ is the average density of overburden strata in kg/m^3 ; g is the acceleration of gravity, N/kg ; H is the mining depth, m ; and σ is the coal strength, MPa .

The stress on pillars (PS_p), pillar strength (S_p), and safety factor (SF_p) after peeling can, thus, be calculated as:

$$PS_p = \rho g H \frac{(w_p + w_c)^2}{(w_p - 2d_m)^2}, \quad (23)$$

$$S_p = \sigma \frac{(w_p - 2d_m)^{0.46}}{h^{0.66}}, \quad (24)$$

$$SF_p = \frac{S_p}{SP_p}, \quad (25)$$

The Salamon formula was based on back-analysis of both stable and failed pillars, but did not consider the peeling progress. Hence, it may underestimate the coal strength σ (7.176 MPa). Since it is very likely that the pillar peels before it collapses, the actual pillar width should be used instead of the nominal pillar width. Therefore, the uniaxial compressive strength (UCS) of coal was utilized to calculate the pillar strength. It should also be noted that the database from South Africa includes some highly joint-influenced coal fields and the coal pillars have very low strength. According to York [16], the strength of these coal pillar can be as low as 40% of the pillar strength in other mining areas. Thus, the database from South Africa was divided into ordinary coal fields (ZA-N) and weak coal fields (with highly-jointed strata, ZA-W). An averaged USC of 21 MPa is used to represent the coal strength for ordinary coal fields in South Africa [33], and 8.4 MPa (40% of 21 MPa) for weak coal fields.

The bulk factor k and the repose angle φ are needed to calculate the peeling depth d_m . The bulk factor of coal is usually 1.05–1.2, and the stronger the coal is the larger the bulk factor will be [34]. The repose angle of non-compacted coal is usually about 27–45° [35] and studies indicated that the angles are affected by the angularity of rock materials, the particle size, and the material inhomogeneity etc. [36,37]. The repose angle or coal debris properties of the collected cases are not provided in the literature; hence, for simplicity, it is assumed that the weak coal is harder to form angular shaped particles and has smaller particle sizes than the stronger coal: the repose angle of coal from ordinary coal seam is assumed to be 40°, while the repose angle of weak coal is assumed to be 30°. The parameters used in Equations (23)–(25) are listed in Table 2.

Table 2. The parameters used in pillar stability analysis.

Area	Pillar Number		$\rho \times 10^3 \text{ (kg/m}^3\text{)}$	$\sigma \text{ (MPa)}$	k	φ
	Failed	Stable				
CN	22	2	2.5	22.7		
IN	14	15	2.1–3.1	21–50	1.2	40
ZA-N	57	317	2.5	21		
ZA-W	52	20	2.5	8.4	1.1	30
Total	145	354	-	-	-	-

Table 3 shows the failed and stable pillar cases in China. Most initial safety factors of failed pillars in China are larger than 1, which is consistent with actual site conditions: these pillars were stable during mining activities, but fail after mine abandonment. The safety factor after peeling in Table 3 shows that only one case is incorrectly computed, and the initial safety factors do not show any pillar collapse. The results from India and South Africa are provided as supplementary materials as they had been provided by other researchers.

Table 4 shows the evaluation accuracy of 145 failed pillars and 354 stable pillars. Pillar failure is time-dependent and stable pillars may still have a danger of collapse in the near future. The evaluation accuracy should refer to the failed pillar cases. To determine the evaluation accuracies, South Africa pillar cases have been studied with classical pillar design methods and pillar peeling model methods: in the classical pillar design method, the Salamon formula with a constant coal strength of 7.2 MPa and a critical safety factor of 1.6 are widely accepted in room-and-pillar mines in South Africa [16]. In the failed pillar cases, if the coal strength is 7.2 MPa, the evaluation accuracy is 26% for weak coal fields, but if the joint effects were considered and the coal strength is reduced to 40% and the accuracy for weak coal fields is improved to 92%, indicating that the strength assumption for weak coal field is acceptable. The evaluation accuracy of classical pillar design method is above 90% for South Africa. The pillar peeling model uses coal USC as the coal strength in the Salamon formula, and a safety factor of 1 as the critical safety factor, the evaluation accuracies of all three countries are above 90%. Therefore, the peeling model is considered acceptable. In stable cases, the evaluation accuracy of peeling model is more than 70% for ordinary coal fields, but is 55% for weak coal fields, this indicated that 27% of Indian pillars, 20% ordinary coal pillars, and 45% weak coal pillars in South Africa still face long-term stability issues.

Table 3. The failed and stable pillar cases in the Yulin Mining Area in China.

No.	Stat.	H (m)	w_p (m)	w_c (m)	h (m)	SF_0	d_m (m)	SF_p	No.	Stat.	H (m)	w_p (m)	w_c (m)	h (m)	SF_0	d_m (m)	SF_p
1	F	115	6	9	5.6	0.9	3.7	0	13	F	140	8	14	5	0.8	3	0
2	F	110	6	8	5	1.2	3.2	0	14	F	120	8	8	4.6	1.8	2.7	0.1
3	F	140	8.4	8	4.7	1.7	2.8	0.1	15	F	175	9	5	2.8	3	1.6	1.1
4	F	190	8.4	8	4.7	1.2	2.8	0.1	16	F	172	6	7	2.5	1.4	1.4	0.3
5	F	180	6	8	2.5	1.2	1.4	0.2	17	F	164	8	8	6.5	1.1	4.1	0
6	F	150	7	7.5	3.5	1.5	2.1	0.2	18	F	190	7	8	3.5	1.1	2.1	0.1
7	F	130	8	7	3.5	2.3	2	0.4	19	F	145	7	7	7.5	1	5.2	0
8	F	140	10	13	6	1.1	3.6	0	20	F	160	8	8	4.5	1.4	2.7	0.1
9	F	150	8	8	4.5	1.5	2.7	0.1	21	F	153	6	8	5	0.9	3.2	0
10	F	117	8	8	6	1.6	3.8	0	22	F	125	8	6	5	2.2	3	0.1
11	F	113	8	6	5	2.4	3	0.1	23	S	145	9	5	2.8	3.7	1.6	1.3
12	F	150	8	7	6.5	1.3	4.1	0	24	S	80	6	4	2	6	1.1	1.9

Note: Stat. for pillar status; F for failed pillar; S for stable pillar.

Table 4. The accuracy of evaluation with different parameters.

Area	Peeling Model		Salamon Formula		
	Failed	Stable	Parameters	Failed	Stable
CN	96%	100%	$\sigma = 22.7$ MPa; SF = 1	20%	100%
IN	93%	73%	$\sigma = 21$ –50 MPa; SF = 1	0	100%
ZA-N	93%	80%	$\sigma = 21$ MPa; SF = 1	0	100%
			$\sigma = 7.2$ MPa; SF = 1.6	95%	79%
ZA-W	98%	55%	$\sigma = 21$ MPa; SF = 1	0	100%
			$\sigma = 8.4$ MPa; SF = 1	0	100%
			$\sigma = 7.2$ MPa; SF = 1.6	26%	90%
			$\sigma = 2.9$ MPa; SF = 1.6	92%	15%

The overall evaluation accuracies between the classical pillar design method and pillar peeling method are similar in South African cases. This indicates that the classical method with a coal strength of 7.2 MPa and a safety factor 1.6 contains the pillar peeling. However, the pillar failure mechanism cannot be revealed by this method, and it is only suitable for South African mining areas. On the contrary, the pillar peeling model can better explain the reason for subsequent failure of initially-stable pillars, and the peeling model uses the coal UCS and a theoretical safety factor of 1 to evaluate pillar stability; thus, it has better applicability for other mining areas. When utilizing the pillar peeling model for long-term pillar stability evaluation, the coal strength σ in Equation (24) should be calibrated by the realistic situation. For example, the ZA-W coal fields (Table 2) were affected by highly-jointed strata, the coal strength for this coal fields was calibrated according to the study [16]. The σ in Equation (24) is recommended to be the long-term coal strength when conducting pillar stability evaluation (e.g., σ is the creep strength if there exists unstable creep behavior; σ is the saturated coal strength if the coal pillar is saturated by water, etc.)

6. Effect of Single Pillar Failure on Surrounding Pillars

Assuming that the overburden strata do not cave in, the square pillars are evenly distributed in the goaf, the working panel is flat, and the effect of a single pillar failure on surrounding pillars is then considered. Figure 5 shows the layout of a room-and-pillar mine site, where the row number of pillars is defined as 1, 2, 3, \dots , i and the column number of pillars is defined as 1, 2, 3, \dots , j .

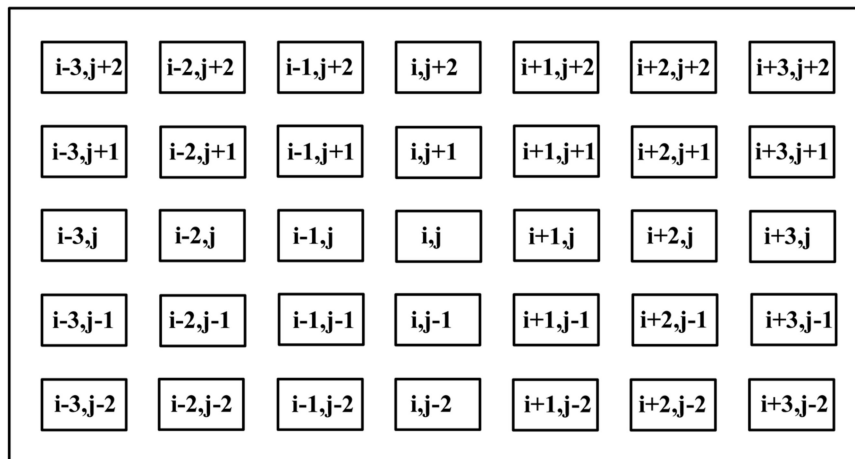


Figure 5. The diagram of the pillar distribution.

We define the pillars $(i-1, j)$, $(i+1, j)$, $(i, j-1)$, and $(i, j+1)$ as the abutted pillars of pillar (i, j) , and pillars $(i-1, j-1)$, $(i-1, j+1)$, $(i+1, j-1)$, and $(i+1, j+1)$ as diagonal pillars of pillar (i, j) . The failure of pillar (i, j) will transfer its load to four abutted pillars and four diagonal pillars; the abutted pillars are the closest pillars to the failed pillar and carry more transferred stress, while the diagonal pillars are further away to the failed pillar and carry less transferred stress. The weight of the transferred stress for a pillar can be calculated by the distance between failed pillar centers and surrounding pillar centers:

$$\frac{4}{w_p + w_c} + \frac{4}{\sqrt{2}(w_p + w_c)} = 1, \quad (26)$$

$$P_{abut} = \frac{1}{w_p + w_c} = \frac{1}{4 + 2\sqrt{2}} = 0.146, \quad (27)$$

$$P_{diag} = \frac{1}{\sqrt{2}(w_p + w_c)} = \frac{1}{4 + 4\sqrt{2}} = 0.104, \quad (28)$$

where P_{abut} and P_{diag} are the weights of the abutting pillar and diagonal pillar, respectively.

When one pillar fails, the stresses on the surrounding pillars are:

$$PS_{abut} = (1 + P_{abut}) \frac{\rho g H (w_p + w_c)^2}{w_p^2}, \quad (29)$$

$$PS_{diag} = (1 + P_{diag}) \frac{\rho g H (w_p + w_c)^2}{w_p^2}, \quad (30)$$

Therefore, if i abutting pillars and j diagonal pillars failed around a pillar, the stress on this pillar (PS_{ij}) and its safety factor (SF_{ij}) are:

$$PS_{ij} = \left(1 + \frac{i}{4 + 2\sqrt{2}} + \frac{j}{4 + 4\sqrt{2}}\right) \frac{\rho g H (w_p + w_c)^2}{w_p^2}, \quad i, j = 0, 1, 2, 3, 4, \quad (31)$$

$$SF_{ij} = \frac{S_0}{SP_{ij}}, \quad (32)$$

Combining Equations (20)–(22) and Equations (31) and (32), the relationship between the initial safety factor and the safety factor after neighboring pillars fail can be calculated as:

$$\frac{SF_{ij}}{SF_0} = \frac{SP_0}{SP_{ij}} = \frac{1}{\left(1 + \frac{i}{4 + 2\sqrt{2}} + \frac{j}{4 + 4\sqrt{2}}\right)}, \quad (33)$$

where i is the number of failed abutting pillars, j is the number of failed diagonal pillars.

Table 5 shows the safety factor for a pillar after its neighboring pillars fail, the effect of diagonal pillar failure is smaller than the effect of abutting pillar failure on a stable pillar. If the initial safety factors of all pillars are 1, any pillar failure will destroy its neighboring pillars. Thus, it results in a likely cascading pillar failure. If the initial safety factor is 1.5, a pillar may still be stable after 50% of its neighboring pillars fail. Table 6 shows the minimum initial safety factor that a pillar can be stable after all of its neighboring pillars fail. If a pillar has an initial safety factor of 2, it will still be stable after losing all of its neighboring pillars. This conclusion befits the historical data from pillar failures in Australia and South Africa well, in which the time-dependent pillar failures appear more frequently when the width–height ratio of pillar is smaller than 4 and the safety factor of the pillar is smaller than 1.5 [14]. Hill [14] also noted that the failed pillars with large width–height ratio ranging from 4 to 8 have safety factors around 0.7–1.5, while the failed pillars with safety factors larger than 2 have a width–height ratio of 2 and below. In the former case, the goaf cannot bear localized pillar failures and cannot prevent the domino-like failures. For the latter case, although the initial safety factor is large enough, the pillar peeling angle is also very large when the width–height ratio is 1–2 (Figure 3). Based on these conclusion, the long-term pillar stability criterion is proposed in Table 7.

Table 5. The safety factor for a pillar after its neighboring pillars fail.

Number of Failed Pillar		Diagonal Pillar ($SF_0 = 1$)					Diagonal Pillar ($SF_0 = 1.5$)				
		0	1	2	3	4	0	1	2	3	4
Abut Pillar	0	1	0.91	0.83	0.76	0.71	1.5	1.36	1.24	1.14	1.06
	1	0.87	0.8	0.74	0.69	0.64	1.31	1.2	1.11	1.03	0.96
	2	0.77	0.72	0.67	0.62	0.59	1.16	1.07	1	0.94	0.88
	3	0.69	0.65	0.61	0.57	0.54	1.04	0.97	0.91	0.86	0.81
	4	0.63	0.59	0.56	0.53	0.5	0.95	0.89	0.84	0.79	0.75

Table 6. The initial safety factor for a stable pillar after its neighboring pillars all fail.

Number of Failed Pillar		Diagonal Pillar				
		0	1	2	3	4
Abut Pillar	0	1.00	1.10	1.21	1.31	1.41
	1	1.15	1.25	1.35	1.46	1.56
	2	1.29	1.40	1.50	1.60	1.71
	3	1.44	1.54	1.65	1.75	1.85
	4	1.59	1.69	1.79	1.90	2.00

Table 7. Long-term stability evaluation and pillar design criterions.

Peeling	Initial Safety Factor	Safety Factor After Peeling	Evaluation
$w_p - 2d_m > 0$	-	≥ 2	Long-term Stable
	-	1.5	Very Stable
	-	1	Stable
	≥ 1	< 1	Stable Temporarily
$w_p - 2d_m \leq 0$	≥ 1	Peeled	
	< 1	-	Failed in Design

7. Conclusions

The long-term stability of coal pillars determines the safety of surface structures and land reutilization in mining areas. Due to the long-term effects of weathering and stressing, the coal pillar will gradually peel off and the reduction of the pillar size increases the possibility of the pillar failure. Thus, it is very important to study the long-term stability of room-and-pillar mines. This paper proposes a non-uniform pillar peeling model for room-and-pillar mining stability evaluation. The validity of the pillar peeling model was verified by 500 stable and failed pillar cases from three countries. The effect of the coal debris pile was investigated by numerical simulation. The effects of single pillar failure on the surrounding pillars were analyzed. Although it is difficult to predict the pillar life, the pillar peeling model considers the worst status of a pillar, providing a preliminary method for the long-term stability evaluation of room-and-pillar mines. The following conclusions can be made:

- (1) The long-term stability of the coal pillar is affected by pillar peeling and pillars with small width–height ratios are more vulnerable to the peeling effect. The pillar size reduction increases the pillar stress and expands the yield zone. However, a stable coal debris pile surrounding a pillar can reduce the yield zone and improve the pillar stability. Additionally, the coal debris pile may protect the pillar rib from the environment, avoiding further weathering on the pillar rib. This means that although the pillar size decreases with time, the pillar size reduction is not limitless, the pillar peeling may not always lead to pillar failures, and the coal debris produced during pillar peeling may stop the pillar from further degradation; on the other hand, this conclusion indicates that the backfill to rooms can improve the pillar stability, and the pillar size can be reduced to improve the recovery ratio of coal resource.
- (2) The peeling damage on the coal pillar can be measured by the peeling angle, which is determined by the width–height ratio. The peeling angle is also affected by the bulk factor and the repose angle of the pile. The maximum peeling depth on the coal pillar is in proportion to the pillar height and tangent to the peeling angle.
- (3) The effects of single pillar failure on the safety factor of the surrounding pillar was discussed, based on which the long-term stability evaluation criteria were proposed for room-and-pillar mining.

Supplementary Materials: The following are available online at <http://www.mdpi.com/1996-1073/10/10/1644/s1>, Table S1: The failed and stable pillar cases in India, Table S2: The failed pillar cases in ordinary coal fields of

South Africa, Table S3: The failed pillar cases in Vaal Basin, Free State and Klip river coal fields of South Africa, Table S4: The stable pillar cases in ordinary coal fields of South Africa, Table S5: The stable pillar cases in Vaal Basin, Free State and Klip river coal fields of South Africa.

Acknowledgments: Financial support is provided by (1) the National Nature Science Fund of China (41604005), and (2) the State Key Laboratory of Geohazard Prevention and Geo-Environment Protection (Chengdu University of Technology) (SKLGP2016K008).

Author Contributions: Ka-zhong Deng provided the main idea of the study; Yang Yu and Hong-dong Fan analyzed the data; Yang Yu wrote the paper; and Shen-en Chen provided language support and revised the paper.

Conflicts of Interest: The authors declare no conflict of interest.

References

1. Mohan, G.M.; Sheorey, P.R.; Kushwaha, A. Numerical estimation of pillar strength in coal mines. *Int. J. Rock Mech. Min.* **2001**, *38*, 1185–1192. [CrossRef]
2. Peng, S.S. *Ground Control Failures: A Pictorial View of Case Studies*; West Virginia University Press: Morgantown, WV, USA, 2007.
3. Shao, X.P.; Shi, P.W.; Wang, H.X. Study on pillars stability by keeping water in strip mining for small and medium-sized mines in northern Shanxi Province. *Coal Technol.* **2009**, *28*, 58–61. (In Chinese)
4. Mathey, M.; Van der Merwe, J.N. Critique of the South African squat coal pillar strength formula. *J. S. Afr. Inst. Min. Metall.* **2016**, *116*, 291–299. [CrossRef]
5. Clarke, B.G.; Welford, M.; Hughes, D.B. The Threat of Abandoned Mines on the Stability of Urban Areas. 2006. Available online: http://iaeg2006.geolsoc.org.uk/cd/papers/iaeg_379.pdf (accessed on 18 November 2016).
6. Luo, Y. Room-and-pillar panel design method to avoid surface subsidence. *Min. Eng.* **2015**, *67*, 105–110.
7. Zipf, R.K. Toward Pillar Design to Prevent Collapse of Room-and-Pillar Mines. 2011. Available online: <https://www.cdc.gov/niosh/mining/UserFiles/works/pdfs/tpdtp.pdf> (accessed on 21 March 2017).
8. Ma, H.; Wang, J.; Wang, Y. Study on mechanics and domino effect of large-scale goaf cave-in. *Saf. Sci.* **2012**, *4*, 689–694. [CrossRef]
9. Dehghan, S.; Shahriar, K.; Maarefvand, P.; Goshtasbi, K. 3-D numerical modelling of Domino failure of hard rock pillars in Fetr6 Chromite Mine, Iran, and comparison with empirical methods. *J. Cent. South Univ.* **2013**, *20*, 541–549. [CrossRef]
10. Li, C.; Xu, J.; Wang, Z.; Qin, S. Domino instability effect of surrounding rock-coal pillars in a room-and-pillar gob. *Int. J. Min. Sci. Technol.* **2013**, *23*, 913–918. [CrossRef]
11. Poulsen, B.A.; Shen, B. Subsidence risk assessment of decommissioned bord-and-pillar collieries. *Int. J. Rock Mech. Min.* **2013**, *60*, 312–320. [CrossRef]
12. Sahu, P.; Lokhande, R.D. An investigation of sinkhole subsidence and its preventive measures in underground coal mining. *Procedia Earth Planet. Sci.* **2015**, *11*, 63–75. [CrossRef]
13. Van der Merwe, J.N. Predicting coal pillar life in South Africa. *J. S. Afr. Inst. Min. Metall.* **2003**, *103*, 293–301.
14. Hill, D. Coal pillar design criteria for surface protection. In Proceedings of the Coal Operators' Conference, University of Wollongong & the Australasian Institute of Mining and Metallurgy, Wollongong, Australia, 26–28 April 2005; pp. 31–38.
15. Van der Merwe, J.N.; Mathey, M. Update of coal pillar database for South African coal mining. *J. S. Afr. Inst. Min. Metall.* **2013**, *113*, 825–840.
16. York, G.; Canbulat, I.; Jack, B.W. Coal Pillar Design Procedures. 2000. Available online: <http://researchspace.csir.co.za/dspace/handle/10204/1419> (accessed on 18 November 2016).
17. Mark, C. The evolution of intelligent coal pillar design: 1981–2006. In Proceedings of the 25th International Conference on Ground Control in Mining, Morgantown, WV, USA, 1–3 August 2006.
18. Biswas, K. Study of Weathering Actions on Partings and Its Effects on Long Term Stability of Coal Pillar. Ph.D. Thesis, West Virginia University, Morgantown, WV, USA, 1997.
19. Castellanza, R.; Gerolymatou, E.; Nova, R. An attempt to predict the failure time of abandoned mine pillars. *Rock Mech. Rock Eng.* **2008**, *41*, 377–401. [CrossRef]
20. Esterhuizen, G.S.; Dolinar, D.R.; Ellenberger, J.L. Pillar strength in underground stone mines in the United States. *Int. J. Rock Mech. Min.* **2011**, *48*, 42–50. [CrossRef]

21. Salmi, E.F.; Nazem, M.; Karakus, M. The effect of rock mass gradual deterioration on the mechanism of post-mining subsidence over shallow abandoned coal mines. *Int. J. Rock Mech. Min.* **2017**, *91*, 59–71. [[CrossRef](#)]
22. Wang, Y.X. Damage Weakening and Fracture Failure Mechanism for Rock Mass Concerning Influence of Water and Initial Defects. Ph.D. Thesis, Central South University, Changsha, China, 2012. (In Chinese)
23. Van der Merwe, J.N. Revised strength factor for coal in the Vaal basin. *J. S. Afr. Inst. Min. Metall.* **1993**, *93*, 71–77.
24. Salamon, M.G.D.; Ozbay, M.U.; Madden, B.J. Life and design of bord-and-pillar workings affected by pillar scaling. *J. S. Afr. Inst. Min. Metall.* **1998**, *98*, 135–146.
25. Wang, H.; Poulsen, B.A.; Shen, B.; Xue, S.; Jiang, Y. The influence of roadway backfill on the coal pillar strength by numerical investigation. *Int. J. Rock Mech. Min.* **2011**, *48*, 443–450. [[CrossRef](#)]
26. Kostecky, T.; Spearing, A.J.S. Influence of backfill on coal pillar strength and floor bearing capacity in weak floor conditions in the Illinois Basin. *Int. J. Rock Mech. Min.* **2015**, *76*, 55–67. [[CrossRef](#)]
27. Li, X.; Kang, T.; Yang, Y.; Li, H.; Li, C.; Wu, L.; Du, M. Analysis of coal wall slip risk and caving depth based on Bishop method. *J. China Coal Soc.* **2015**, *40*, 1498–1504. (In Chinese)
28. Fang, X.Q.; He, J.; Li, H.C. A study of the rib of mechanism in soft coal and its control at a fully-mechanized top-coal caving face. *J. China Univ. Min. Technol.* **2009**, *38*, 640–644. (In Chinese)
29. Huang, Q.X.; Liu, J.H. Vertical slice model for coal wall spalling of large mining height longwall face in shallow seam. *J. Min. Safety Eng.* **2015**, *32*, 187–191. (In Chinese)
30. Shi, B. Study on Influence Factors of Water Conservation Mining in Shallow Seam Mine Area in the North Shaanxi Province. Ph.D. Thesis, Xi'an University of Science and Technology, Xi'an, China, 2012. (In Chinese)
31. Liu, Y.X. Comprehensive evaluation of stability of residual coal-pillar after room-and-pillar mining. *Coal Min. Technol.* **2013**, *18*, 78–80. (In Chinese)
32. Jaiswal, A.; Shrivastva, B.K. Numerical simulation of coal pillar strength. *Int. J. Rock Mech. Min.* **2009**, *46*, 779–788. [[CrossRef](#)]
33. Mathey, M. Investigation into the Mechanism of Strength and Failure in Squat Coal Pillars in South Africa. Ph.D. Thesis, University of the Witwatersrand, Johannesburg, South Africa, 2015.
34. He, G.Q.; Yang, L.; Ling, G.D.; Jia, F.C.; Hong, D. *Mine Subsidence Science*; China University of Mining and Technology Press: Xuzhou, China, 1994. (In Chinese)
35. Tang, M.K. *Introduction of Mining Engineering*; Metallurgical Industry Press: Beijing, China, 2011. (In Chinese)
36. Froehlich, D.C. Mass angle of repose of open-graded rock riprap. *J. Irrig. Drain. Eng.* **2011**, *137*, 454–461. [[CrossRef](#)]
37. Wang, J.; Zhao, D.; Liang, Y.; Wen, H. Angle of repose of landslide debris deposits induced by 2008 Sichuan Earthquake. *Eng. Geol.* **2013**, *156*, 103–110. [[CrossRef](#)]

